Korean J Physiol Pharmacol
Vol 13: 511−516, December, 2009
DOI: 10.4196/kjpp.2009.13.6.511

Cytotoxic Activity and Three-Dimensional Quantitative Structure Activity Relationship of 2-Aryl-1,8-naphthyridin-4-ones

Yong Jin Kim, Eun Ae Kim, Mi Lyang Chung, and Chaeuk Im

College of Pharmacy, Chung-ang University, Seoul 156-756, Korea

A series of substituted 2-arylnaphthyridin-4-one analogues, which were previously synthesized in our laboratory, were evaluated for their *in vitro* cytotoxic activity against human lung cancer A549 and human renal cancer Caki-2 cells using MTT assay. Some compounds (11, 12, and 13) showed stronger cytotoxicity than colchicine against both tumor cell lines, and compound 13 exhibited the most potent activity with IC_{50} values of 2.3 and 13.4 μM, respectively. Three-dimensional quantitative structure activity relationship (3D-QSAR) studies of comparative molecular field analysis (CoMFA) and comparative molecular similarity indices analysis (CoMSIA) were performed. Predictive 3D-QSAR models were obtained with q^2 values of 0.869 and 0.872 and r^2_{ncv} values of 0.983 and 0.993 for CoMFA and CoMSIA, respectively. These results demonstrate that CoMFA and CoMSIA models could be reliably used in the design of novel cytotoxic agents.

Key Words: CoMFA, CoMSIA, Cytotoxicity, MTT, QSAR

INTRODUCTION

The microtubules play an important role in mitosis. Compounds that attack microtubules can inhibit or promote microtubule assembly, resulting in cell arrest in mitosis (Jordan and Wilson, 2004). Therefore, these antimitotic compounds have been used as anticancer drugs. For example, vinca alkaloids inhibit tubulin polymerization into microtubules and taxoids promote microtubule assembly (Rowinsky and Donehower, 1992; Verwij et al., 1994). Colchicine is another antimitotic agent, but it is not used clinically due to its high toxicity (Hastie, 1991; Chen et al., 1997).

Some flavonoid derivatives interfere with tubulin polymerization to produce potent cytotoxic activity against several cancer cell lines (Shi et al., 1995; Manthey et al., 2001). To find more potent antimitotic compounds, some researchers have synthesized new flavonoid analogues, such as 2-arylquinolin-4-ones (Xia et al., 1998; Lai et al., 2005; Nakamura et al., 2005), 2-arylnaphthyridin-4-ones (Chen et al., 1997; Zhang et al., 1999), and 2-arylquinazolin-4-ones (Hamel et al., 1996; Hour et al., 2000; Xia et al., 2001). Some of these compounds, especially 2-arylnaphthyridin-4-ones, exhibit potent cytotoxicity; thus, we synthesized a series of substituted 2-arylnaphthyridin-4-one analogues and conducted cytotoxicity assays in human tumor cell lines (Chung, 2004).

The 3D-QSAR model yields some information about the structural requirements for more potent activity of ligands when the structure of the receptor is not known (Rieger et al., 2001). In this paper, we report the cytotoxic activity and 3D-QSAR analysis of sixteen synthesized compounds to further the development of more potent cytotoxic agents.

Received November 25, 2009, Revised December 3, 2009, Accepted December 17, 2009

Corresponding to: Chaeuk Im, College of Pharmacy, Chung-ang University, Heuksuk-dong, Dongjak-gu, Seoul 156-756, Korea. (Tel) 82-2-820-5603, (Fax) 82-2-816-7338, (E-mail) Chaeukim@cau.ac.kr

METHODS

Materials

Phosphate-buffered saline (PBS) was purchased from Boehringer Mannheim (Indianapolis, IN). 3-[4,5-dimethylthiazol-2-yl]-2,5-diphenyltetrazolium bromide (MTT), colchicine, trypsin, dimethyl sulfoxide (DMSO), and other reagents were purchased from Sigma (St. Louis, MO). Human lung cancer A549 and renal cancer Caki-2 tumor cell lines were obtained from Chong Kun Dang Pharmaceutical Corp., and 2-aryl-1,8-naphthyridin-4-one analogues were synthesized in our laboratory.

In vitro cytotoxic assay

The prepared compounds were tested for their cytotoxicity against the human lung cancer A549 and human renal cancer Caki-2 cell lines. The cytotoxic activity was determined using a MTT-based colorimetric assay. Briefly, cell lines were seeded at a density of approximately 5×10^3 cells/well in 96-well plates. Each well contained 180 μl of medium to which 20 μl of 10×concentration of the prepared compounds or PBS were added. After 4 days of culture,

ABBREVIATIONS: 3D-QSAR, three dimensional quantitative structure activity relationship; PBS, phosphate-buffered saline; MTT, 3-[4,5-dimethylthiazol-2-yl]-2,5-diphenyltetrazolium bromide; CoMFA, comparative molecular field analysis; CoMSIA, comparative molecular similarity indices analysis.

0.1 mg of MTT was added to each well and incubated at 37°C for 4 h. Plates were centrifuged at 450×g to precipitate the formazan crystals. The medium was removed and 150 μl of DMSO was added to each well to dissolve formazan. In this assay, MTT was converted to blue formazan by mitochondrial enzymes. The intensity of the blue color formed was measured with an ELISA reader at 540 nm. The IC_{50} value was defined as the concentration of the compound that reduced the absorbance at 540 nm by 50% (Park et al., 1987; Manthey and Guthrie, 2002).

Molecular modeling and alignment

A total of sixteen compounds exhibiting cytotoxic activity with IC_{50} values ranging from 2.3~276.5 μM were used to perform the 3D-QSAR analysis. The IC_{50} values were transformed into pIC_{50} ($-\log IC_{50}$) values and used as the dependent variable in CoMFA and CoMSIA studies. The structures of the training set and the test set are shown in Table 1. The data set was divided into two groups. Thirteen compounds (1~13) were used for the training set. Three compounds (T1~T3) were selected randomly as a test set and were used for external validation of the 3D-QSAR models.

Molecular modeling was performed using the Sybyl 8.1.1 software of Tripos (SYBYL, 2009). All molecules were sketched by the sketch module in SYBYL. Each structure was optimized using a conjugate gradient method based on the TRIPOS force field with Gasteiger Huckel charges and gradient convergence criteria of 0.05 kcal/mol. Simulated annealing on the energy optimized structures was carried out with 50 cycles. They were heated at 1000 K for 1000 fs to reach equilibrium and then annealed at 200 K for 1000 fs. The 50 conformations were then minimized to obtain low energy conformations for each compound. The structures were aligned by using the align database. Compound (13), which showed the most potent activity, was selected as a template molecule. The 1,8-naphthyridin fragment of compound (13) in its optimized conformation was used as a common substructure in the alignment.

CoMFA and CoMSIA

CoMFA and CoMSIA analysis are based on the relationships between biological activity and structural properties of the compounds when the receptor structure is not known. In the CoMFA study, the aligned molecules were put in a three-dimensional grid of 2A°. The steric and electrostatic properties of the compounds were calculated at each grid point using Lennard-Jones potential and Coulombic potential, respectively. The sp^3 carbon probe atom with +1 charge and Van der Waals radius of 1.52A° were used to calculate the CoMFA steric and electrostatic fields. The default value of 30 kcal/mol was used as the maximum steric and electrostatic energy cut-off. In CoMSIA analysis, five fields are calculated: steric, electrostatic, hydrophobic, hydrogen bond acceptor, and hydrogen bond donor fields. The probe atoms with radius 1A°, charge +1, hydrophobicity +1, hydrogen bond donating +1, and hydrogen bond accepting +1 were used to calculate the five fields. The attenuation factor of 0.3 was used as the default value.

The partial least squares (PLS) were carried out using the cross-validated leave one out (LOO) method to evaluate q^2 values. The model of highest q^2 value and lowest standard error of prediction suggested the optimum number of components. Leave one out (LOO) cross-validation was used to estimate the predictive ability of the models (Jackson et al., 2009).

Table 1. *In vitro* cytotoxic activity of 2-aryl-1,8-naphthyridin-4-ones compared with colchicines

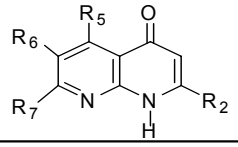

Compound	R_5	R_6	R_7	R_2	Cytotoxicity IC_{50} (μM)	
					A549	Caki-2
1	H	H	H	3',4'-dimethoxy phenyl	194.6	276.5
2	CH_3	H	CH_3	3',4'-dimethoxy phenyl	115.7	183.9
3	H	Cl	H	3',4'-dimethoxy phenyl	105.2	138.5
4	CH_3	H	H	3',4'-dimethoxy phenyl	25.7	129.7
T1	H	CH_3	H	3',4'-dimethoxy phenyl	95.0	121.8
5	H	H	CH_3	3',4'-dimethoxy phenyl	84.9	116.1
6	H	H	H	2',4'-dimethoxy phenyl	98.5	146.8
7	CH_3	H	CH_3	2',4'-dimethoxy phenyl	99.0	113.8
8	CH_3	H	H	2',4'-dimethoxy phenyl	102.1	111.2
T2	H	CH_3	H	2',4'-dimethoxy phenyl	69.5	112.3
9	H	H	CH_3	2',4'-dimethoxy phenyl	64.2	103.5
T3	H	H	H	naphthyl	93.1	100.3
10	CH_3	H	CH_3	naphthyl	139.9	50.7
11	CH_3	H	H	naphthyl	9.4	19.1
12	H	CH_3	H	naphthyl	10.9	17.5
13	H	H	CH_3	naphthyl	2.3	13.4
Colchicine					56.0	21.2

RESULTS

In vitro cytotoxic activity

The sixteen synthesized compounds and colchicine were evaluated for their cytotoxicity *in vitro* against lung cancer A549 and renal cancer Caki-2 cells. The cytotoxic activities of each compound were obtained as IC_{50} values, and the data are presented in Table 1. Colchicine showed moderate cytotoxicity with IC_{50} values of 56 and 21.2 μM against A549 and Caki-2 tumor cell lines in our assay conditions, respectively. Among the synthesized compounds, Compounds 11, 12, and 13 showed stronger cytotoxic activity than colchicine against both tumor cell lines. They have a naphthyl group at the C_2-position in 1,8-naphthyridine and showed IC_{50} values of 9.4, 10.9, and 2.3 μM against lung cancer A549 cells and 19.1, 17.5, and 13.4 μM against renal cancer Caki-2 cells, respectively. The compound 13 gave the most potent activity and its IC_{50} values were 2.3 and 13.4 μM, respectively. The IC_{50} values of the other compounds ranged from 25.7 to 194.6 μM in A549 cells and 50.7 to 276.5 μM in Caki-2 cells.

CoMFA and CoMSIA analysis

The statistical data from CoMFA and CoMSIA models are shown in Table 2.

Lung cancer A549: By use of CoMFA default settings with steric and electrostatic fields, a cross-validated coefficient (q^2)=0.820 with 3 optimum number of components (N) was observed. This model had a non-cross-validated coefficient (r^2_{ncv})=0.983, standard error of estimate (SEE)= 0.092, and F value=115.575. CoMFA with only steric field showed q^2=0.869, N=3, r^2_{ncv}=0.983, SEE=0.091, and F value= 118.709. Six CoMSIA models were calculated from the same training and test sets. CoMSIA model with only steric field gave q^2 value=0.863, N=3, r^2_{ncv}=0.977, SEE=0.107, and F value=83.623. These statistical parameters indicate the accuracy of model.

CoMFA model with steric field showed higher q^2 value (0.869) than any other CoMFA and CoMSIA models. Therefore, using this model, the predicted pIC_{50} values for each training set and the residual were calculated (Table 3). The predicted pIC_{50} values of the test set molecules and their residual values are shown in Table 4. These test set compounds were used to validate CoMFA model with steric field. A graph of the predicted pIC_{50} values versus actual pIC_{50} values for the training set and test set is shown in Fig. 1A.

Renal cancer Caki-2 cells: Six CoMSIA models with steric, electrostatic, hydrogen bond acceptor, and hydrogen bond donor fields were considered. In the CoMSIA model with steric and electrostatic fields, a cross-validated coefficient (q^2)=0.872, optimum number of components (N)=3, non-cross-validated coefficient (r^2_{ncv})=0.993, standard error of estimate (SEE)=0.042, and F value=305.023 were observed. CoMFA model with electrostatic field gave q^2=0.838, N=4, r^2_{ncv}=0.984, SEE=0.064, and F value=126.912.

Table 2. Statistical data of CoMFA and CoMSIA for two tumor cell lines

Field[a]	q^{2b}	N[c]	SEP[d]	r^2_{ncv}[e]	SEE[f]	F[g]	Contributions[a]			
							S	E	D	A
Lung cancer A549										
CoMFA										
S	**0.869**	**3**	**0.240**	**0.983**	**0.091**	**118.709**	**1**			
E	0.266	1	0.514	0.962	0.138	50.095		1		
SE	0.820	3	0.281	0.983	0.092	115.575	0.843	0.157		
CoMSIA										
S	0.863	3	0.245	0.977	0.107	83.623	1			
E	0.255	1	0.518	0.950	0.158	37.767		1		
D	0.806	2	0.277	0.940	0.173	31.115			1	
A	0.306	4	0.586	0.956	0.148	43.137				1
SE	0.577	4	0.457	0.977	0.108	83.536	0.491	0.509		
DA	0.799	2	0.282	0.931	0.184	27.051			0.413	0.587
Renal cancer Caki-2										
CoMFA										
S	0.412	1	0.338	0.989	0.054	184.305	1			
E	0.838	4	0.208	0.984	0.064	126.912		1		
SE	0.715	3	0.260	0.992	0.046	248.683	0.637	0.363		
CoMSIA		1	0.372	0.976	0.080	81.450				
S	0.287						1			
E	0.827	3	0.202	0.985	0.062	135.235		1		
D	0.538	2	0.314	0.946	0.120	35.053			1	
A	0.485	4	0.371	0.948	0.118	36.104				1
SE	**0.872**	**3**	**0.174**	**0.993**	**0.042**	**305.023**	**0.319**	**0.681**		
DA	0.619	3	0.301	0.916	0.150	21.837			0.323	0.677

[a]Fields used, S, steric; E, electrostatic; D, H-bond donor; A, H-bond acceptor; [b]q^2, cross-validated correlation coefficient from leave-one-out(LOO); [c]N, optimum number of components; [d]SEP, standard error of prediction; [e]r^2_{ncv}, non-crossvalidated correlation coefficient; [f]SEE, standard error of estimate; [g]F, F-test value.

Table 3. Actual and predicted activity (pIC_{50}) of training set

Compound	A549			Caki-2		
	Actual	Predicted	Residual	Actual	Predicted	Residual
1	3.71	3.78	−0.07	3.56	3.64	−0.08
2	3.94	3.86	0.08	3.74	3.69	0.05
3	3.98	3.90	0.08	3.86	3.82	0.04
4	4.59	4.59	0.00	3.89	3.89	0.00
5	4.07	4.16	−0.09	3.94	3.94	0.00
6	4.01	3.94	0.07	3.83	3.82	0.01
7	4.00	4.08	−0.08	3.94	3.96	−0.02
8	3.99	3.94	0.05	3.95	3.92	0.03
9	4.19	4.29	−0.10	3.99	4.01	−0.02
10	3.85	3.81	0.04	4.30	4.29	0.01
11	5.03	5.09	−0.06	4.72	4.76	−0.04
12	4.96	5.00	−0.04	4.76	4.76	0.00
13	5.64	5.53	0.11	4.87	4.84	0.03
	Average		0.07			0.03

Table 4. Actual and predicted activity (pIC_{50}) of test set

Compound	A549			Caki-2		
	Actual	Predicted	Residual	Actual	Predicted	Residual
T1	4.02	3.85	0.17	3.91	3.94	−0.03
T2	4.16	4.00	0.16	3.95	4.01	−0.06
T3	4.03	3.95	0.08	4.00	4.39	−0.39
	Average		0.14			0.16

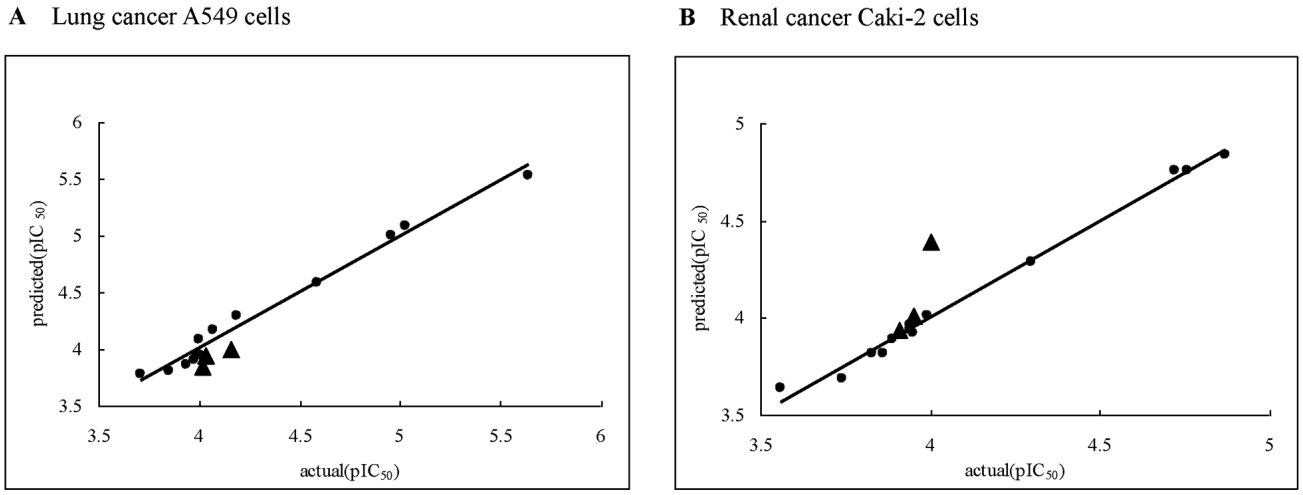

Fig. 1. Scatter plot of actual activities versus predicted activities against A549 (A) and Caki-2 (B) tumor cell lines (●: training set molecules, ▲: test set molecules).

CoMSIA model with steric and electrostatic fields showed better q^2 value (0.872) than any other CoMFA and CoMSIA models. With this model, the predicted pIC_{50} values for the training set and the residuals were calculated (Table 3). The predicted pIC_{50} values of the test set and their residual values are shown in Table 4. The graph of predicted pIC_{50} values versus actual pIC_{50} values for the training set and test set is shown in Fig. 1B.

DISCUSSION

2-Phenyl-4-quinolones reportedly act as antimitotic agents that interact with tubulin at the colchicine site (Kuo et al., 1993; Li et al., 1994). The 2-phenyl-1,8-naphthyridin-4-ones can be considered isosteres of 2-phenyl-4-quinolones. Since the CH moiety in 4-quinolone is isosterically substituted to nitrogen atom at the C_8-position in 1,8-naph-

thyridin-4-one, the 2-phenyl-1,8-naphthyridin-4-one can be assumed to have similar biological activity to 2-phenyl-4-quinolones.

In terms of average cytotoxicity in the A549 tumor cell line, compounds with methyl substituted at the C_6-position were less active than those substituted at the C_5 or C_7-position in the 1,8-naphthyridin ring, while compounds with two methyl groups at both the C_5 and C_7-positions or no substituted group at the C_5, C_6 and C_7-positions in 1,8-naphthyridin were substantially less active. In renal cancer Caki-2 cells, methyl-substituted compounds at the C_7-position were more potent than those substituted at the C_5 or C_6-position in 1,8-naphthyridin, while methyl substituted compounds at both C_5 and C_7-positions or no substituted group at C_5, C_6 and C_7-positions in 1,8-naphthyridin were much less active.

The effects of substitutions at the C_5, C_6 and C_7-positions depend on the substitution at the C_2-position in 1,8-naphthyridin, which is consistent with the previously reported trend (Chen et al., 1997). The introduction of a naphthyl group at C_2-position increased cytotoxicity and methoxy substituted compounds at both the C_2`and $C_4$`-positions were more active than those substituted at the C_3`and $C_4$`-positions in 1,8-naphthyridin.

A CoMFA contour map of steric fields in lung cancer A549 cells

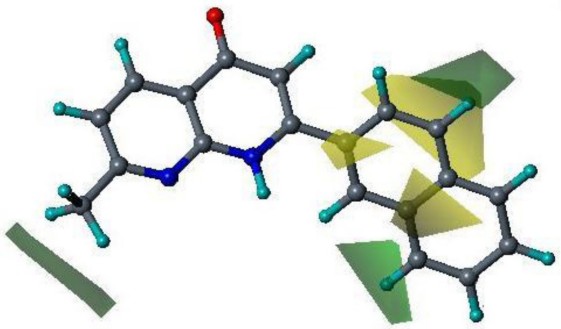

B CoMSIA contour map of steric and electrostatic fields in renal cancer Caki-2 cells

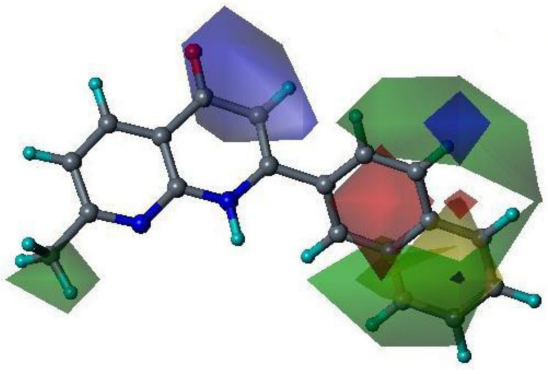

Fig. 2. Contour maps of steric and electrostatic fields in lung cancer A549 (A) and renal cancer Caki-2 (B) cells. Compound 13 is shown inside the field. Color-coding is as follows: Green indicates regions where bulky groups increase activity, whereas yellow indicates regions where bulky groups decrease activity. Blue indicates that positive charge favors high activity, whereas red indicates that negative charge favors high activity.

For lung cancer A549 cells, the statistical results from the CoMFA model with steric field demonstrated high cross-validated value q^2 (0.869) and non-cross-validated coefficient value r^2_{ncv} (0.983), and these values suggest that this model was predictive. In general, a q^2 value higher than 0.5 is considered an indication that the model is internally predictive. This model showed optimum component number=3 and suggested that steric interaction strongly influenced the cytotoxic activity.

For renal cancer Caki-2 cells, the CoMSIA model with steric and electrostatic fields showed higher q^2 value than CoMFA models. Good predictivity of the model was indicated by high q^2 (0.872) and r^2_{ncv} (0.993) coefficient values. The relative contributions of steric field (31.9%) and electrostatic field (68.1%) indicated that strong electrostatic interaction was involved in the activity.

The small average residual values (0.07 and 0.03) of actual and predicted activities in Table 3 indicated that the predicted activities from CoMFA and CoMSIA models correlated well with actual activities. The test set was used to validate the predictivity of these CoMFA and CoMSIA models. The residual values of the test set were calculated and their small average residual values (0.14 and 0.16) demonstrated that the predicted values of the test set also correlated well with the actual values.

Contour maps indicate the regions around molecules where increased or decreased activity was predicted by physicochemical property changes in the molecules. The CoMFA contour map of steric field in lung cancer A549 cells and the CoMSIA contour maps of steric and electrostatic fields in renal cancer Caki-2 cells are shown in Fig. 2. In the steric contour map, the green contours indicate sterically favored regions, whereas the yellow contours designate sterically unfavorable regions. In the electrostatic contour map, blue and red regions are favorable for positive charge and negative charge, respectively. The molecule in the contour maps is compound (13), which showed the most potent activity.

The CoMFA steric contour map in lung cancer A549 cells (Fig. 2A) illustrated two small yellow contours above the C_2-naphthyl ring and one large yellow contour below the C_2-naphthyl ring of 1,8-naphthyridin. These steric contours indicate that bulky substituents at these sites are unfavorable for cytotoxic activity. This yellow contour map suggests that a flat phenyl or naphthyl ring at the C_2-position increases cytotoxic activity, but non-flat and bulky substituents at the C_2-position decrease cytotoxicity. The presence of green contours at the C_4` and $C_8$`-positions of the naphthyl ring and near the methyl group at the C_7-position in 1,8-naphthyridin indicates that bulky groups around these regions increase the cytotoxic activity. This green contour map proposes that atoms bigger than hydrogen at the C_4` and $C_8$`-position of the naphthyl ring and that groups bigger than methyl at the C_7-position of 1,8-naphthyridin might increase the activity.

The CoMSIA steric contour map in renal cancer Caki-2 cells (Fig. 2B) displayed sterically favorable green regions at the C_3`, $C_4$`, C_7`, and $C_8$`-positions of the C_2-naphthyl ring and the methyl group at the C_7-position in 1,8-naphthyridin. This green contour map suggests that the in-

troduction of bulky groups in these areas might increase the cytotoxic activity against renal cancer Caki-2 cells. The presence of a sterically unfavorable yellow region above the C_2-naphthyl ring indicates that bulky groups around these regions decrease the cytotoxic activity, but a flat naphthyl ring at the C_2-position is acceptable for the activity. The CoMSIA electrostatic contour map in renal cancer Caki-2 cells (Fig. 2B) showed the favorable regions for positive charge (blue) near the C_3 and C_4-position of 1,8-naphthyridin and the C_4`-position of the C_2-naphthyl ring. These blue contours indicate that electron-deficient groups at these sites enhance the cytotoxic activity, and the carbonyl group in the C_4-position of 1,8-naphthyridin might be important for activity. The presence of a red contour in the C_2-naphthyl ring suggests that negative electrostatic potential around this region increases the cytotoxic activity, and the electron-rich C_2- naphthyl ring increases the activity.

In summary, compounds 11, 12, and 13 produced stronger cytotoxicity than colchicine against both tumor cell lines. The good predictivity of the CoMFA and CoMSIA models was shown by high q^2 (0.869 and 0.872) and r^2_{ncv} (0.983 and 0.993) coefficient values. The small average residual values of the training (0.07 and 0.03) and test (0.14 and 0.16) sets indicated that the predicted activities from the CoMFA and CoMSIA models correlated well with the actual activity. The CoMFA contour map in lung cancer A549 cells suggested that atoms bigger than hydrogen at the C_4` and $C_8$`-positions of the naphthyl ring and groups bigger than methyl at the C_7-position of 1,8-naphthyridin might increase the cytotoxicity. The CoMSIA contour map in renal cancer Caki-2 cells suggested that the introduction of bulky groups at the C_3`, $C_4$`, C_7`, and $C_8$`-positions of the C_2-naphthyl ring and the C_7-position in 1,8-naphthyridin and that positively charged groups near the C_3 and C_4-positions of 1,8-naphthyridin and the C_4`-position of the C_2-naphthyl ring might enhance the cytotoxic activity. In addition, the carbonyl group in the C_4-position and the C_2-naphthyl ring of 1,8-naphthyridin might be important for biological activity.

ACKNOWLEDGEMENTS

This Research was supported by the Chung-Ang University Research Grants in 2009.

REFERENCES

Chen K, Kuo SC, Hsieh MC, Mauger A, Lin CM, Hamel E, Lee KH. Antitumor agents. 174. 2′,3′,4′,5,6,7-Substituted 2-phenyl-1,8-naphthyridin-4-ones: their synthesis, cytotoxicity, and inhibition of tubulin polymerization. *J Med Chem* 40: 2266−2275, 1997.

Chung ML. Synthesis and Anti-Cancer Activity of 2-Phenyl-1,8-naphthyridine-4-one Derivatives. Chung Ang Graduate School Master thesis, 2004.

Hamel E, Lin CM, Plowman J, Wang HK, Lee KH, Paull KD. Antitumor 2,3-Dihydro-2-(aryl)-4(1*H*)-quinazolinone Derivatives. Interactions with Tubulin. *Biochem Pharmacol* 51: 53−59, 1996.

Hastie SB. Interaction of colchicine with tubulin. *Pharmacol Ther* 51: 377−401, 1991.

Hour MJ, Huang LJ, Kuo SC, Xia Y, Bastow K, Nakanishi Y, Hamel E, Lee KH. 6-Alkylamino- and 2,3-dihydro-3′-methoxy-2-phenyl-4-quinazolinones and related compounds: their synthesis, cytotoxicity, and inhibition of tubulin polymerization. *J Med Chem* 43: 4479−4487, 2000.

Jackson PL, Scott KR, Southerland WM, Fang YY. Enaminones 8: CoMFA and CoMSIA studies on some anticonvulsant enaminones. *Bioor Med Chem* 17: 133−140, 2009.

Jordan MA, Wilson L. Microtubules as a target for anticancer drugs. *Nat Rev* 4: 253−264, 2004.

Kuo SC, Lee HZ, Juang JP, Lin YT, Wu TS, Chang JJ, Lednicer D, Paull KD, Lin CM, Hamel E, Lee KH. Synthesis and cytotoxicity of 1,6,7,8-substituted 2-(4′-substituted-phenyl)-4-quinolones and related compounds: Identification as antimitotic agents interacting with tubulin. *J Med Chem* 36: 1146−1156, 1993.

Lai YY, Huang LJ, Lee KH, Xiao Z, Bastow KF, Yamori T, Kuo SC. Synthesis and biological relationships of 3′,6-substituted 2-phenyl-4-quinolone-3-carboxylic acid derivatives as antimitotic agents. *Bioorg Med Chem* 13: 265−275, 2005.

Li L, Wang HK, Kuo SC, Wu TS, Lednicer D, Lin CM, Hamel E, Lee KH. Antitumor agents. 150. 2′,3′,4′,5′,5,6,7-Substituted 2-phenyl-4-quinolones and related compounds: Their synthesis, cytotoxicity, and inhibition of tubulin polymerization. *J Med Chem* 37, 1126−1135, 1994.

Manthey JA, Guthrie N. Antiproliferative Activities of Citrus Flavonoids against Six Human Cancer Cell Lines. *J Agric Food Chem* 50: 5837−5843, 2002.

Manthey JA, Guthrie N, Grohmann K. Biological properties of citrus flavonoids pertaining to cancer and inflammation. *Curr Med Chem* 8: 135−153, 2001.

Nakamura S, Kozuka M, Bastow KF, Tokuda H, Nishino H, Suzuki M, Tatsuzaki J, Morris Natschke SL, Kuo SC, Lee KH. Cancer preventive agents, part 2: synthesis and evaluation of 2-phenyl-4-quinolone and 9-oxo-9,10-dihydroacridine derivatives as novel antitumor promoters. *Bioorg Med Chem* 13: 4396−4401, 2005.

Park JG, Kramer BS, Steinberg SM, Carmichael J, Collins JM, Minna JD, Gazdar AF. Chemosensitivity testing of human colorectal carcinoma cell lines using a tetrazolium-based colorimetric assay. *Cancer research* 47: 5875−5879, 1987.

Rieger JM, Brown ML, Sullivan GW, Linden J, and Macdonald TL. Design, Synthesis, and Evaluation of Novel A2A Adenosine Receptor Agonists. *J Med Chem* 44: 531−539, 2001.

Rowinsky EK, Donehower RC. The clinical pharmacology and use of antimicrotubule agents in cancer chemotherapeutics. *Pharmacol Ther* 52: 35−84, 1992.

Shi Q, Chen K, Li L. Antitumor Agents. 154. Cytotoxic and antimitotic flavonols from *Polanisia dodecandra*. *J Nat Prod* 58: 475−482, 1995.

SYBYL Molecular Modeling Software. Tripos Inc., St. Louis, USA, 2009.

Verwij J, Clavel M, Chevalier B. Paclitaxel (Taxol) and docetaxel (Taxotere): Not simply two of a kind. *Ann Oncol* 5: 495−505, 1994.

Xia Y, Yang ZY, Hour MJ, Kuo SC, Xia P, Bastow KF, Nakanishi Y, Nampoothiri P, Hackl T, Hamel E, Lee KH. Antitumor agents. Part 204: Synthesis and biological evaluation of substituted 2-arylquinazolinones. *Bioorg Med Chem Lett* 11: 1193−1196, 2001.

Xia Y, Yang ZY, Xia P, Bastow KF, Tachibana Y, Kuo SC, Hamel E, Hackl T, Lee KH. Antitumor Agents. 181. Synthesis and Biological Evaluation of 6,7,2′,3′,4′-Substituted-1,2,3,4-tetrahydro-2-phenyl-4-quinolones as a New Class of Antimitotic Antitumor Agents. *J Med Chem* 41: 1155−1162, 1998.

Zhang SX, Bastow KF, Tachibana Y, Kuo SC, Hamel E, Mauger A, Narayanan VL, Lee KH. Antitumor agents. 196. Substituted 2-thienyl-1,8-naphthyridin-4-ones: their synthesis, cytotoxicity, and inhibition of tubulin polymerization. *J Med Chem* 42: 4081−4087, 1999.